

# Linewidths for magnetic precession driven by DC spin-polarized currents

J. C. Sankey, I. N. Krivorotov, S. I. Kiselev, P. M. Braganca, N. C. Emley, R. A. Buhrman, and D. C. Ralph  
*Cornell University, Ithaca, NY, 14853 USA*

We analyze the temperature dependence of linewidths for resistance oscillations associated with magnetic precession driven by spin-transfer torques. We argue that the linewidths are dominated at low temperature by thermal deflections of the magnetization about its equilibrium trajectory, and at high temperature by thermally-activated transitions between dynamical modes. Simple macrospin simulations predict wider linewidths from thermal deflections than we observe and also less ubiquitous thermal activation, which suggests that spatially non-uniform magnetic dynamical modes are relevant.

PACS numbers: 85.75.-d, 75.75.+a, 76.50.+g

Recent experiments have shown that a spin-polarized DC current can drive microwave-frequency precession in nanometer-scale magnetic multilayers [1-4], in agreement with predictions [5,6]. The magnetic motions produce GHz-frequency oscillations of the sample resistance  $R(t)$  that, when measured with a spectrum analyzer, give peaks in the microwave power density vs. frequency (Fig. 1(a)). The peaks have non-zero widths, indicating that the oscillations are not perfectly periodic. For potential applications such as nanoscale microwave sources and magnetic oscillators, it is advantageous to minimize the linewidths, which have varied significantly in previous experiments. For samples in a nanopillar geometry, full-widths-at-half-maxima (FWHM) in power as narrow as 550 MHz have been reported for Co layers at room temperature [1] while Py ( $\text{Ni}_{81}\text{Fe}_{19}$ ) layers at 40 K have yielded FWHMs as small as 6.4 MHz [4]. Linewidths less than 2 MHz have been observed for excitations within extended (unpatterned) Py films in point-contact devices at room temperature [2]. Here we investigate the processes that govern the linewidths of spin-transfer-driven microwave signals. We argue that two mechanisms contribute: thermal deflections of the magnetic moment about its equilibrium trajectory and thermally-activated transitions out of the precessional state.

We focus on devices having a nanopillar geometry (Fig. 1(a) inset). The samples are composed of sputtered metal multilayers fabricated into elliptical cross-sections using the procedure of ref. [1]. The devices that we examine have different sequences of layers (noted below), but all contain one thin Py "free" layer (2-7 nm thick) that can be driven into precession by spin-transfer torques and a thicker or exchange-biased "fixed" Py layer that polarizes the current and does not undergo dynamics in the current range we discuss. These layers are separated by a Cu spacer. When biased with a DC current ( $I$ ), precession of the free-layer magnetic moment results in a microwave signal  $IR(t)$ , which we amplify and measure with a spectrum analyzer. Figure 1(b) is a dynamical phase diagram for Device 1 determined from microwave measurements as in ref. [1], with magnetic field ( $H$ ) applied in the sample plane along the magnetically easy axis. This device has the layer structure 80 nm Cu / 20 nm Py / 6 nm Cu / 2 nm Py / 2 nm Cu / 30 nm Pt, with an approximately elliptical cross-section of 120 nm  $\times$  60 nm, and a resistance of 6  $\Omega$ . We will focus in this paper on dynamical states near bias points corresponding to the dot in Fig. 1(b) where, as a function of increasing  $I$ , the sample evolves from a configuration in which the moments of the two magnetic layers are parallel (P), to a dynamical mode with small-angle precession (SD), to a mode with larger-angle precession (LD).

Figure 2(a) shows the measured temperature dependence of the FWHM of the peak in power density observed at twice the fundamental precession frequency in Device 1 [7]. Because the linewidth depends on the magnitude of the precession angle  $\theta$  measured in plane (see inset, Fig. 2(a)), as temperature ( $T$ ) is changed we keep the average precession angle  $\langle\theta\rangle$  approximately constant. For Device 1, we do this by monitoring the power in the second harmonic, estimating  $\langle\theta\rangle$  using the procedure of ref. [1], and adjusting  $I$  between 1.1 mA (25 K) and 0.9 mA (170 K) to fix  $\langle\theta\rangle$  near an estimated value of 32°, where the linewidth is a minimum in this device. The misalignment angle between the precession axis and the fixed layer magnetization (as estimated from the first and second harmonic [1]) is  $\theta_{\text{mis}} \sim 2^\circ$ . The measured linewidth is strongly dependent on  $T$ , increasing by a factor of 5 between 25 K and 170 K. We have observed qualitatively similar behavior in 6 samples, throughout the region of the phase

diagram where precessional excitations are observed. Figure 2(b) shows results near the fundamental precession frequency for smaller-angle precession in Device 2, composed of 80 nm Cu / 20 nm Py / 10 nm Cu / 7 nm Py / 20 nm Cu / 30 nm Pt, with cross-section 130 nm  $\times$  40 nm, and resistance 20  $\Omega$ . These data correspond to  $\langle\theta\rangle$  small enough that the second-harmonic signal is not resolvable [8], so we control  $\langle\theta\rangle$  by monitoring the power in the fundamental peak, and estimate  $\langle\theta\rangle < 12^\circ$ . The strong  $T$  dependence that we observe in all samples indicates that thermal effects determine the linewidths above 25 K.

In order to analyze these results, we first consider the simplest model, in which the magnetic moment of the free layer is assumed to respond as a single macrospin. The magnetic dynamics can then be determined by integrating the Landau-Lifshitz-Gilbert (LLG) equation of motion with the Slonczewski form of the spin-transfer torque [9]. Thermal effects are modeled by a randomly fluctuating field  $\mu_0 H_{th}$ , with each spatial component drawn from a Gaussian distribution of zero mean and standard deviation  $\sqrt{2\alpha k_B T / \gamma M_s V \Delta t}$ , where  $\alpha$  is the Gilbert damping parameter,  $k_B$  is Boltzmann's constant,  $\gamma$  is the gyromagnetic ratio,  $M_s$  and  $V$  are the magnetization and volume of the free layer, and  $\Delta t$  is the integration time step [10,11]. Theoretical studies of this model have been performed previously [12-17]. Thermal fluctuations displace the free-layer moment both (a) along and (b) transverse to the precessional path. Fluctuations along the precessional path speed and slow the moment's progress, directly inducing a spread in precession frequency  $f$ . From the time needed for this random-walk process to produce dephasing, we estimate the contribution to the FWHM from this mechanism to be

$$\Delta f_a \approx \frac{4\pi\gamma\alpha k_B T}{M_s V D^2} n^2, \quad (1)$$

where  $D$  is the length of the precession trajectory on the unit sphere, and  $n = 1$  or  $2$  for the first or second harmonic peak. If we substitute parameters appropriate for Device 1:  $\alpha = 0.025$  [4],  $T = 150$  K,  $\mu_0 M_s = 0.81$  T [18],  $n = 2$ , dimensions  $2 \times 120 \times 60$  nm $^3$ , and  $\theta = 32^\circ$ , we predict a contribution from this mechanism of  $\Delta f_a \approx 12$  MHz. This is much less than the measured linewidths at  $T = 150$  K, and the linear  $T$  dependence also differs from the experiment, so we conclude that the contribution from this mechanism is likely negligible for our samples. The second mechanism, (b) thermal fluctuations of the free-layer moment transverse to the precessional path, will produce fluctuations in  $\theta$  about  $\langle\theta\rangle$  (upper inset, Fig. 3). If  $f$  depends on  $\theta$ , this will cause an additional spread  $\Delta f_b$ . Different regimes are possible for the resulting linewidths, depending on the magnitude of  $df/d\theta$ , the width of the distribution in  $\theta$ , and the correlation time for fluctuations in  $\theta$ . However, LLG simulations suggest that our data correspond to a simple regime (long correlation times) in which the linewidth is simply proportional to the FWHM  $\Delta\theta$  of the distribution of precession angles weighted by the magnitude of the resistance oscillations associated with each value of  $\theta$  [19]:

$$\Delta f_b = n \frac{df}{d\theta} \bigg|_{\langle\theta\rangle} \Delta\theta. \quad (2)$$

The triangles in Fig. 3 display values of the right-hand side of Eq. (2), with  $\Delta\theta$  and

$df / d\theta|_{\langle\theta\rangle} \approx 35$  MHz/degree both determined from a LLG simulation. The parameters used in the simulation are those corresponding to Device 1 (listed above), together with an in-plane uniaxial anisotropy  $\mu_0 H_k = 20$  mT, an out-of-plane anisotropy  $\mu_0 M_{\text{eff}} = 0.8$  T [18],  $I = 1.2$  mA, and  $\mu_0 H = 50$  mT applied along the easy axis, with the fixed layer moment in the same direction. We assume that the angular dependence of the Slonczewski torque is simply proportional to  $\sin(\theta)$  with an efficiency parameter of 0.2 [16]. The squares in Fig. 3 show the FWHM calculated directly from the Fourier transform of  $R(t)$  obtained in the same simulation. The agreement in Fig. 3 demonstrates that Eq. (2) gives a good description of the linewidths expected from LLG dynamics within the macrospin approximation.

The temperature dependence of the calculated linewidths in Fig. 3 is to good accuracy  $T^{1/2}$  at low  $T$  (inset, Fig. 3). This is the form that follows from Eq. (2) if one assumes that Boltzmann statistics can be applied approximately to describe the distribution of  $\theta$  in this non-equilibrium problem. If fluctuations of  $\theta$  about  $\langle\theta\rangle$  are subject to an effective linear restoring term (which will depend on the angular dependencies of the damping and spin-transfer torques), then both simulations and simple analytical calculations show that  $\Delta\theta \approx AT^{1/2}$ , where  $A$  is a constant. Deviations from  $T^{1/2}$  are seen for  $T > 15$  K, where  $\Delta\theta$  becomes large enough that the restoring term is no longer linear.

Consider now the data for Device 1 shown in Fig. 2(a). Over the temperature range 25 - 110 K, we can make a reasonable fit using Eq. (2) with the approximation that  $\Delta\theta \approx AT^{1/2}$ , using the single variable parameter  $A df / d\theta|_{\langle\theta\rangle} = 2.3$  MHz K $^{-1/2}$ .

However, the measured widths are approximately a factor of eight narrower than those predicted by the macrospin simulation with parameters chosen to model this sample (Fig. 3). The measured value  $df / d\theta|_{\langle\theta\rangle} \sim 30$  MHz/degree is similar to the simulation, so the

effective linear restoring term required to model our device ( $\propto 1/A^2$ ) would have to be larger by a factor of  $\sim 50$ . We have not been able to account for so large a difference by varying device parameters over a reasonable range or by employing different predictions for the angular dependence of the spin torque [9]. We are therefore led to the surprising suggestion that spatially non-uniform dynamical modes may generate narrower linewidths at low  $T$  than are possible within the macrospin approximation.

Above  $T \approx 120$  K, the measured linewidths (Fig. 2) increase with  $T$  much more rapidly than the approximate  $T^{1/2}$  dependence predicted by the macrospin LLG model. A plausible mechanism for the strong  $T$  dependence is thermally-activated switching between different dynamical magnetic modes, leading to linewidths inversely proportional to the lifetime of the precessional state. Switching between steady-state precessional modes and static states has previously been identified at frequencies from  $< 100$  kHz [18,20,21] to 2 GHz [22]. The consequences on linewidths have been considered previously within LLG simulations [16]. To estimate the effects of such switching, we assume that the average lifetime of a precessional state has the form  $\tau \approx (1/f) \exp(E_b / k_B T)$ , where  $E_b$  is an effective activation barrier. The Fourier transform then yields a linewidth

$$\Delta f_{sw} = \frac{1}{\pi\tau} = \frac{f}{\pi} \exp(-E_b/k_B T). \quad (3)$$

We find that the combination of Eqs. (2) and (3) gives a good description of the strong  $T$  dependence of the linewidths in Fig. 2(a) and 2(b) using the fitting parameter  $E_b/k_B = 400$  K for Device 1 and is 880 K for Device 2. Note that Eq. (3) alone would predict low- $T$  linewidths much smaller than we measure. The effective barriers from the fits are small compared to the static anisotropy barrier  $\mu_0 M_s H_k V/k_B \sim 10,000$  K in Device 1 and 100,000 K in Device 2, indicating that the barriers for switching between the dynamical states are distinct from simple macrospin magnetic anisotropies [22].

Direct evidence for the importance of the switching mechanism can be seen in some samples (e.g., Device 3, composition 80 nm Cu / 8 nm IrMn / 4 nm Py / 8 nm Cu / 4 nm Py / 20 nm Cu / 30 nm Pt, with a cross section  $130 \times 60$  nm<sup>2</sup> and a resistance of 11  $\Omega$ ) for which, at particular values of  $I$ ,  $H$ , and  $T$ , multiple peaks can appear simultaneously in the power spectrum at frequencies that are not related harmonically (Fig. 4). In these regimes, the widths of both peaks are broader than when only a single mode is visible in the spectrum. We suggest the cause is rapid mode switching between two different dynamical states.

Within macrospin simulations at the experimental temperatures, we do not find high-frequency switching between metastable states except in narrow regions of the dynamical phase diagram where nearly-degenerate modes exist [14,16]. In contrast, experimentally we observe strong thermally-activated temperature dependence whenever precessional dynamics are present, for  $T > 120$  K. We suspect that the ubiquity of the thermally-activated transitions is further evidence for a breakdown of the macrospin approximation, and that the observed switching is due to transitions between non-uniform magnetization modes [23,24]. Micromagnetic simulations might help to reveal the true nature of the dynamics in this interesting regime.

The overall picture of the linewidths suggested by our data is that they are dominated by thermal fluctuations of the precession angle at low  $T$ , and thermally-activated mode switching at high  $T$  or near bias points where two or more different modes are accessible. The narrowest linewidths that we have achieved for free-layer oscillations in nanopillar devices (5.2 MHz at 40 K, Fig. 1(a), for a sample composition the same as Device 3) are observed in devices containing an antiferromagnetic layer to exchange-bias the fixed magnetic layer 45° relative to the easy axis. We speculate that the reduced symmetry brought about by exchange biasing may decrease the thermally-activated component of the linewidth by reducing the probability of near degeneracies in low-energy modes.

We thank J. Xiao and M. Stiles for helpful discussions. We acknowledge support from DARPA through Motorola, from the Army Research Office, and from the NSF/NSEC program through the Cornell Center for Nanoscale Systems. We also acknowledge NSF support through use of the Cornell Nanofabrication Facility/NNIN and the Cornell Center for Materials Research facilities.

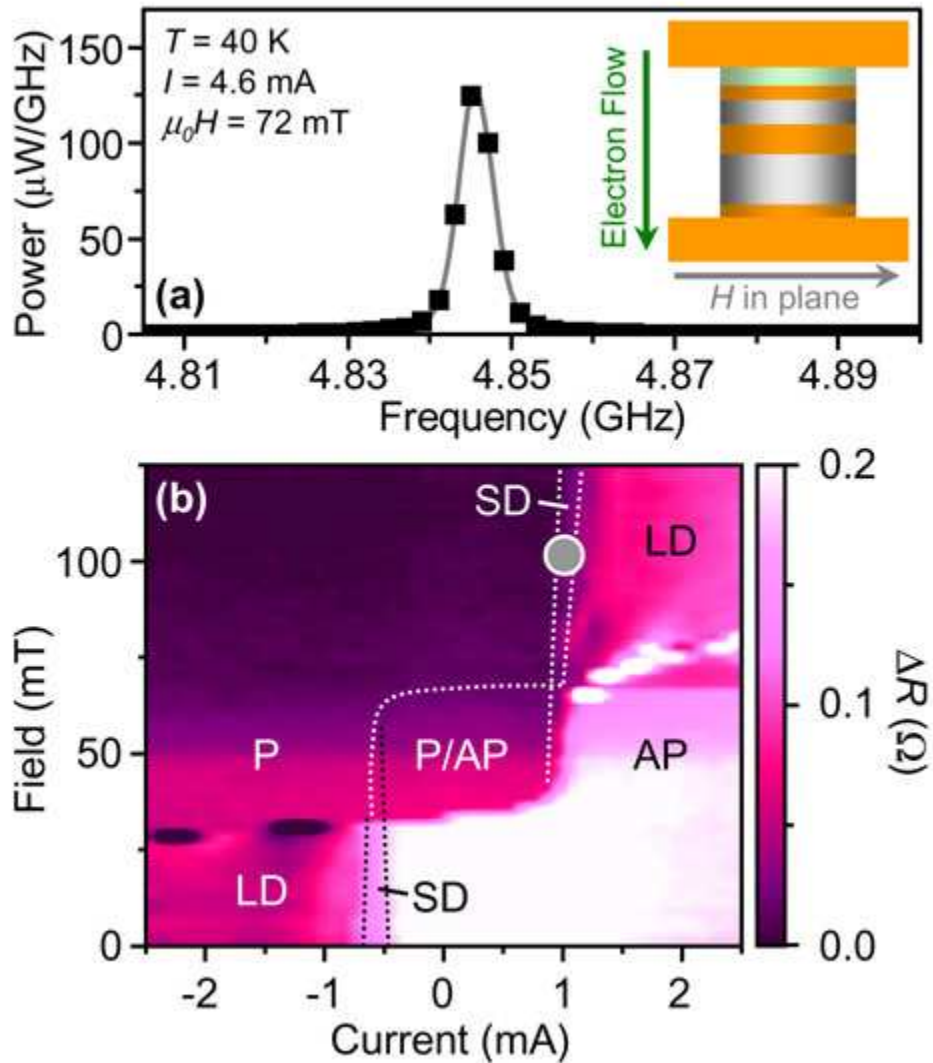


FIG. 1 (Color online) (a) The narrowest spectral peak for free-layer oscillations that we have observed in a nanopillar (FWHM = 5.2 MHz). The device has the same composition as Device 3, described in the text. (inset) Schematic of a nanopillar device. Positive current denotes electron flow from the free to the fixed magnetic layer. (b) Differential resistance of Device 1 as a function of  $I$  and  $H$  at  $T = 4.2$  K, obtained by increasing  $I$  at fixed  $H$ . AP denotes static antiparallel alignment of the two magnetic moments, P parallel alignment, P/AP a bistable region, SD small-angle dynamics, and LD large-angle dynamics.

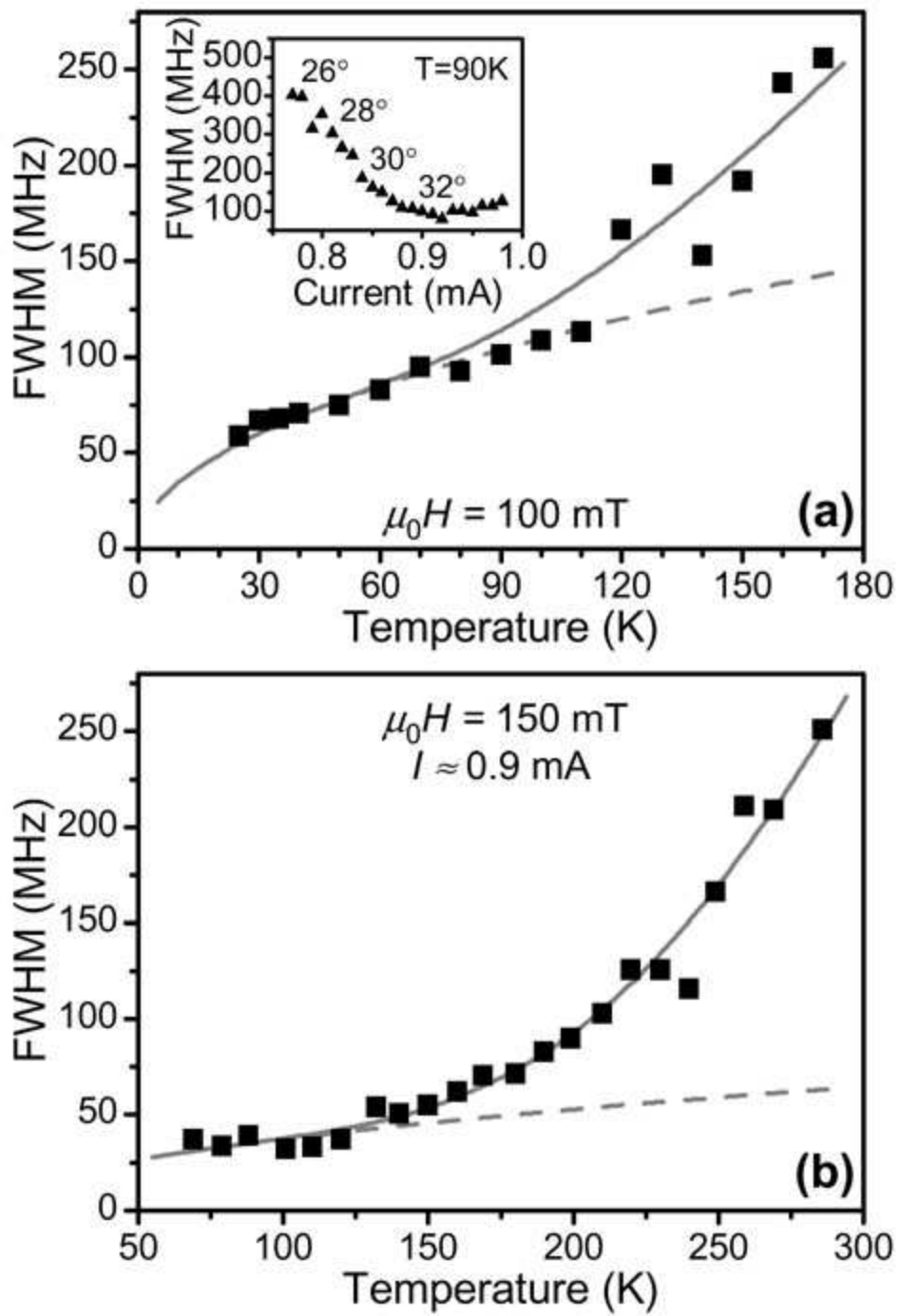


FIG. 2 Measured linewidths vs.  $T$  for (a) Device 1 and (b) Device 2. The dashed line is a fit of the low- $T$  data to Eq. (2) and the solid line is a combined linewidth from Eqs. (2) and (3), obtained by convolution. (inset) Dependence of linewidth on  $I$  for Device 1, with estimates of precession angles.

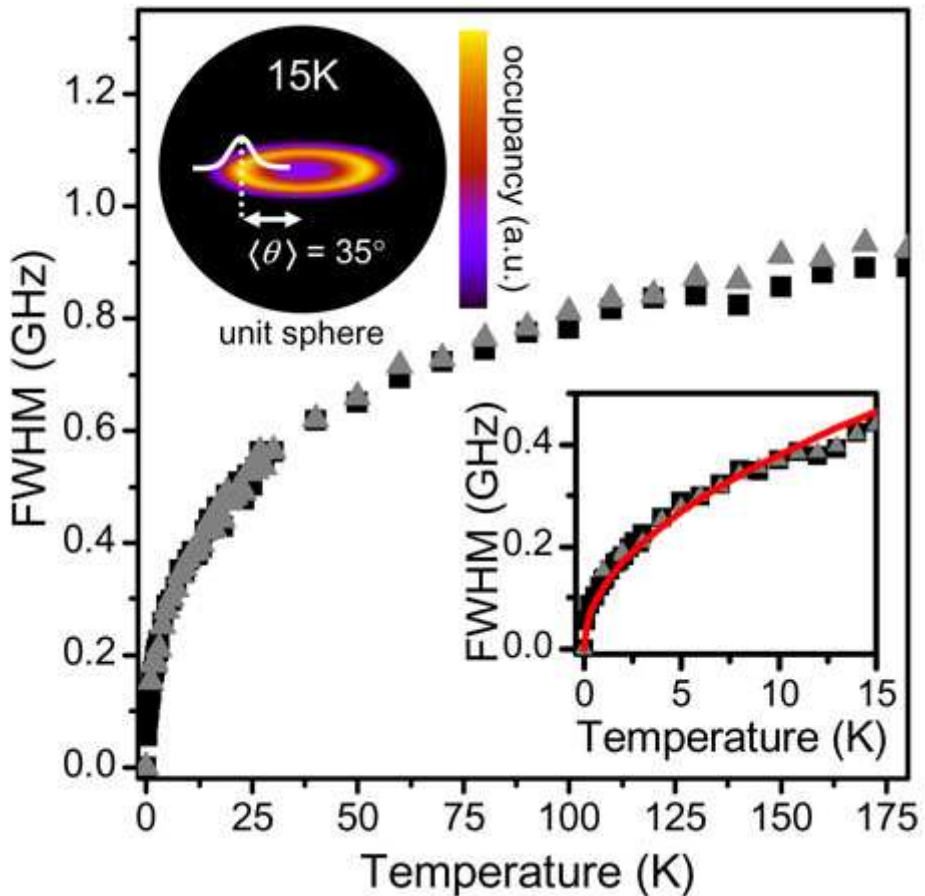


FIG. 3 (Color online) (Main plot and lower inset) Squares: Linewidth calculated directly from the Fourier transform of  $R(t)$  within a macrospin LLG simulation of the dynamics of Device 1. Triangles: Linewidth calculated from the same simulation using the right-hand side of Eq. (2). Line in inset: Fit to a  $T^{1/2}$  dependence. (Top inset) Simulated probability distribution of the precession angle at 15 K.

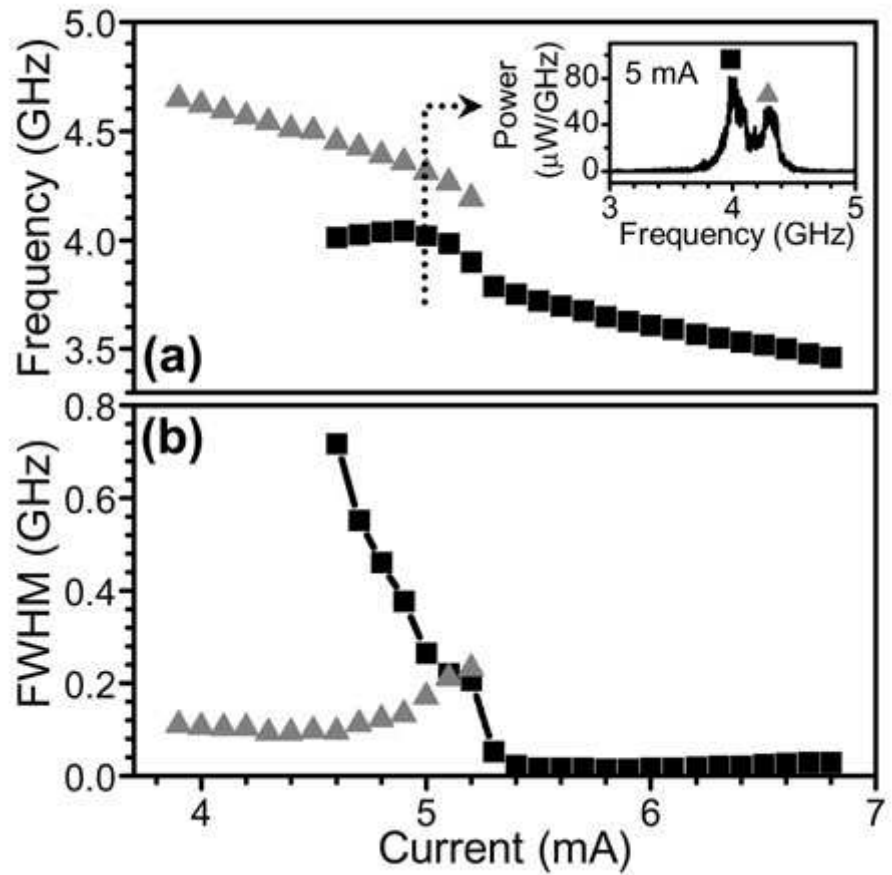


FIG. 4 Measured (a) frequencies and (b) linewidths of modes in Device 3 for  $T = 40$  K,  $\mu_0 H = 63.5$  mT applied in the exchange bias direction,  $45^\circ$  from the free-layer easy axis. When two modes are observed in the spectrum simultaneously, both linewidths increase.

## References

- [1] S. I. Kiselev *et al.*, *Nature* **425**, 380 (2003).
- [2] W. H. Rippard *et al.*, *Phys. Rev. B* **70**, 100406(R) (2004); *Phys. Rev. Lett.* **92**, 027201 (2004).
- [3] S. I. Kiselev *et al.*, *Phys. Rev. Lett.* **93**, 036601 (2004).
- [4] I. N. Krivorotov *et al.*, *Science* **307**, 228 (2005).
- [5] J. C. Slonczewski, *J. Magn. Magn. Mater.* **159**, L1 (1996).
- [6] L. Berger, *Phys. Rev. B* **54**, 9353 (1996).
- [7] The linewidths for Device 1 approach a constant value below  $\sim$ 20 K, as expected due to ohmic heating. See the heating estimate in ref. [17].
- [8] The fundamental peak is more prominent in Device 2 because  $\theta_{\text{mis}}$  is larger than in Device 1.
- [9] J. Xiao, A. Zangwill, and M. D. Stiles, *Phys. Rev. B* **70**, 172405 (2004).
- [10] W. F. Brown, *Phys. Rev.* **130**, 5 (1963).
- [11] R. H. Koch, J. A. Katine, and J. Z. Sun, *Phys. Rev. Lett.* **92**, 088302 (2004).
- [12] J. Z. Sun, *Phys. Rev. B* **62**, 570 (2000).
- [13] J. Grollier *et al.*, *Phys. Rev. B* **67**, 174402 (2003).
- [14] Z. Li and S. Zhang, *Phys. Rev. B* **68**, 024404 (2003).
- [15] Y. B. Bazaliy, B. A. Jones, and S. C. Zhang, *Phys. Rev. B* **69**, 094421 (2004).
- [16] S. E. Russek *et al.*, *Phys. Rev. B* **71**, 104425 (2005).
- [17] J. Xiao, A. Zangwill, and M. D. Stiles, *cond-mat/0504142*.
- [18] I. N. Krivorotov *et al.*, *Phys. Rev. Lett.* **93**, 166603 (2004).
- [19] For small angles, this weighting is  $\propto \theta_{\text{mis}}^2 \theta^2$  for the fundamental peak and  $\propto \theta^4$  for the second harmonic; see the online supporting material in ref. [4].
- [20] S. Urazhdin *et al.*, *Phys. Rev. Lett.* **91**, 146803 (2003).
- [21] A. Fábián *et al.*, *Phys. Rev. Lett.* **91**, 257209 (2003).
- [22] M. R. Pufall *et al.*, *Phys. Rev. B* **69**, 214409 (2004).
- [23] M. D. Stiles, J. Xiao, and A. Zangwill, *Phys. Rev. B* **69**, 054408 (2004).
- [24] M. L. Polianski and P. W. Brouwer, *Phys. Rev. Lett.* **92**, 26602 (2004).